Труды Москов. Матем. Общ.
Том 79 (2018), вып. 2

Trans. Moscow Math. Soc.
2018, Pages 209–229
https://doi.org/10.1090/mosc/284
Article electronically published on November 29, 2018

# BIFURCATIONS OF THE 'HEART' POLYCYCLE IN GENERIC 2-PARAMETER FAMILIES

A. V. DUKOV

Abstract. The paper concerns the 'heart' polycycle. We show that the set of vector fields containing a 'heart' polycycle form a Banach submanifold of codimension two in the space of smooth vector fields on a two-dimensional sphere. The bifurcation diagram of a generic family containing such a polycycle is constructed and surgery on the phase portrait is described.

## 1. Introduction

We consider a vector field on a sphere which contains a 'heart' polycycle (see Figure 1.1) consisting of two saddle points joined by separatrix connections.

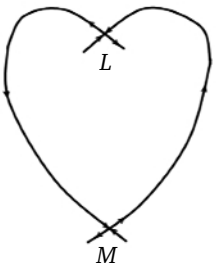


Figure 1.1. The 'heart' polycycle.

We will investigate the question of semilocal bifurcation of such a 'heart' in a generic 2-parameter family. The bifurcation being semilocal means that it is studied only in a small neighbourhood of the polycycle. Consider the bifurcation diagram of the family. Under a 'natural' choice of parameters described below, interesting bifurcations only occur in the first quadrant, for positive values of the parameters. Possible bifurcation diagrams are shown in Figures (1.2a) and (1.2b).

The curves $SL_1$ and $SL_2$ correspond to the separatrix loops. In Figure (1.2a), the curve $PC$ corresponds to a parabolic cycle. The countable set of curves accumulating at $PC$ and $SL_1$ corresponds to the so-called sparkling separatrix connections. The bifurcation under scrutiny is the simplest semilocal bifurction where sparkling separatrix connections occur.

A sparkling separatrix connection in a one-parameter family is a parameter-dependent sequence of separatrix connections between the same two saddles, each one making a greater number of turns than the previous one. They were discovered by Malta and Palis in 1981. In [2] they described a one-parameter family in which a bifurcation of the parabolic limit cycle occurs. The separatrices of the saddles wind around this limit

2010 *Mathematics Subject Classification.* Primary 34C23, 34C37, 37J45.
*Key words and phrases.* polycycle, two-parameter family, bifurcation diagram, sparkling separatrix.

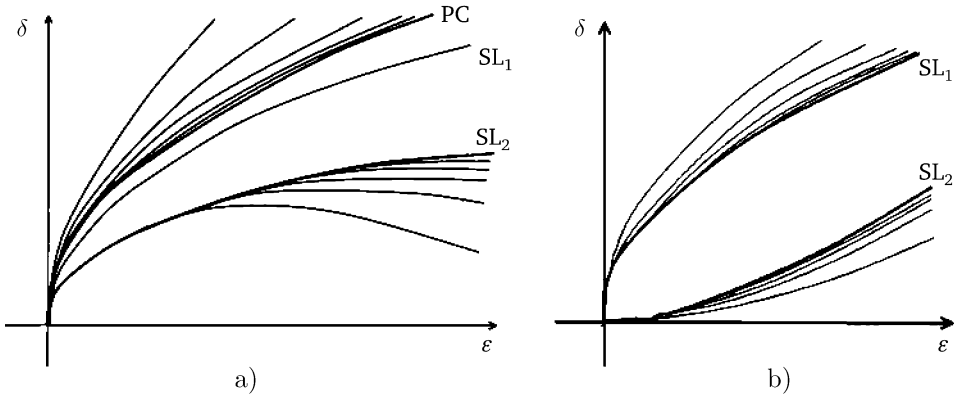


FIGURE 1.2. Two possible bifurcation diagrams.

cycle from both sides, forming sparkling separatrix connections when the cycle breaks up. Recently it was shown in [4] that sparkling connections are not only of independent interest: the simultaneous appearance of several series of connections in a family can lead to the appearance of a numerical invariant, a quantity which does not change when passing to equivalent families. The only cases that have been looked at up to now have been global bifurcations, where the sparkling connections are due to external saddles (remote from the bifurcating polycycle or cycle). In 2015, Yu.S. Il'yashenko raised the question: Are sparkling separatrix connections to be found in generic semilocal families? This article gives a positive answer to this question.

Recall that the *characteristic exponent of a saddle* is the ratio of its eigenvalues taken with a minus sign and with the negative eigenvalue on the numerator. The saddle is called dissipative if its characteristic exponent is greater than 1. There exist two qualitatively different scenarios of the 'heart' polycycle bifurcation, depending on the dissipativity of the saddle points. The key result of this paper is presented in the following two theorems.

**Theorem 1.** *For dissipative and non-dissipative saddles, the bifurcation diagram of a generic 2-parameter family which perturbs a vector field with a 'heart' polycycle is the union of curves approaching the origin comprising two curves corresponding to the vector fields with a separatrix loop, one curve corresponding to the vector field with a parabolic limit cycle and two infinite sets of curves corresponding to the sparkling separatrix connections.*

The bifurcation diagram for this case is shown in Figure 8.1.

**Theorem 2.** *The bifurcation diagram for a generic 2-parameter family perturbing a vector field with a 'heart' polycycle is, in the case of two non-dissipative saddles, is a union of curves tending to the origin, comprising two curves corresponding to the vector fields with separatrix loops and two infinite series of curves corresponding to the sparkling separatrix connections.*

The bifurcation diagram in this case is shown in Figure 8.2. All the necessary definitions are given in Section 2, together with all the main concepts and notation used throughout the paper. The main object of study is a generic 2-parameter family of vector fields on a sphere. Each parameter of the family is defined as the unlocking threshold of the respective connection. The vector field contains a 'heart' polycycle when the parameters are zero. This section also contains the definition of the Poincaré map which we need to find the limit cycles.

Section 3 is devoted to the geometry of vector fields with a 'heart' polycycle in the space of all vector fields. Such fields form a smooth Banach submanifold of codimension 2.

Sections 4–7 are mainly concerned with giving a description of the bifurcation diagram of the family. We will show that on the diagram there is a countable set of curves going out from the origin of the coordinate base of the parameters. These curves correspond to vector fields with separatrix connections or a semistable limit cycle. In particular, we will prove the existence of sparkling separatrix connections.

## 2. The 'heart' polycycle and its Poincaré map

Consider a $C^1$-smooth 2-parameter family $V$ of vector fields on a sphere with parameters $\varepsilon$ and $\delta$. Suppose that for any values of the parameters the vector fields of the family contain two saddles $M(\varepsilon,\delta)$ and $L(\varepsilon,\delta)$. Exactly how the parameters are defined is described below.

Let $\mu$ and $\lambda$ be the characteristic exponents of the saddles $M$ and $L$, respectively; these depend on the parameters of the family. We assume that the vector field corresponding to zero parameters is generic:

$$\mu(0),\lambda(0)\notin\mathbb{Q},\quad \lambda(0)\mu(0)\neq 1. \tag{1}$$

We also assume that when both parameters are zero there are two separatrix connections between the saddles which constitute a polycycle, that is, in this case, a digon with vertices at the saddle points $M$ and $L$ and the separatrices as the edges. Moreover, the free separatrices (not involved in its formation) are located on different sides of the polycycle. In what follows, we will use the term 'separatrix' only for those separatrices which participate in the formation of the polycycle, that is, those that constitute the separatrix connection when the parameters are zero (see Figure 1.1).

We draw transversals $\Gamma_1^+,\Gamma_1^-,\Gamma_2^+,\Gamma_2^-$ to the polycycle as follows. We assume that $\Gamma_1^+$ and $\Gamma_1^-$ are located within a neighbourhood $U_M$ of the saddle $M$ which will be defined below, and the separatrix approaching the saddle $M$ intersects $\Gamma_1^+$, while the one leaving it intersects $\Gamma_1^-$. The transversals $\Gamma_2^+,\Gamma_2^-$ are located near the saddle $L$ in a similar way.

We choose coordinates on these transversals, with the origin at the point of intersection of the separatrix from the nearest saddle with the transversal and such that the orientation of the transversals $\Gamma_1^+,\Gamma_1^-$ is opposite to the orientation of the transversals $\Gamma_2^+,\Gamma_2^-$ with respect to the polycycle (see Figure 2.1).

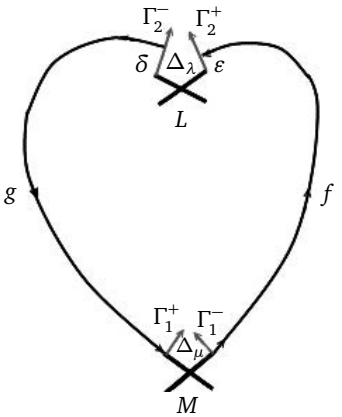


Figure 2.1. A perturbed 'heart' polycycle.

According to [1] (Chapter 9, 1.2) and the genericity condition (1), for certain neigbourhoods $U_M$ and $U_L$ of the saddles $M$ and $L$ there exist finitely-smooth coordinates on the transversals such that the transition maps in a neighbourhood of zero are of the form:

$$\Delta_\lambda : \Gamma_2^+ \to \Gamma_2^-, \qquad \Delta_\lambda(x,\varepsilon,\delta) = x^{\lambda(\varepsilon,\delta)}; \tag{2}$$

$$\Delta_\mu : \Gamma_1^+ \to \Gamma_1^-, \qquad \Delta_\mu(x,\varepsilon,\delta) = x^{\mu(\varepsilon,\delta)}. \tag{3}$$

In these coordinates, the point $x = 0$ corresponds to the intersection point of the transversal and separatrix of the corresponding saddle.

We now introduce the parameter-dependent Poincaré map $\Delta$ of a circuit around the whole polycycle:

$$\Delta : \Gamma_1^- \to \Gamma_1^-, \quad \Delta(x) = \Delta(x,\varepsilon,\delta) = \Delta_\mu \circ g \circ \Delta_\lambda \circ f(x). \tag{4}$$

It is defined near the point $x = 0$ for appropriate nonzero values of the parameters and is the composition of the functions (2), (3) with two regular maps, $f : \Gamma_1^- \to \Gamma_2^+$ and $g : \Gamma_2^- \to \Gamma_1^+$ both of which are $C^1$-smooth in a neigbourhood of zero.

Consider an annulus $U \subset \mathbb{S}^2$, which is a neighbourhood of the polycycle for zero values of the parameters, and such that its closure $\bar{U}$ does not contain any limit cycles or other singular points. We suppose that the boundary of $U$ consists of arcs of phase curves of the vector field for zero values of the parameters and of transversals to separatrices that do not form the polycycle. In addition, we assume that the annulus $U$ is sufficiently narrow, so the Poincaré map is defined at each point $U \cap \Gamma_1^-$. Our goal is to study the behaviour of the vector field in this annulus (see Figure 2.2). Notice that the separatrices which do not participate in the formation of the polycycle leave the neighbourhood $U$ (see Figure 2.2).

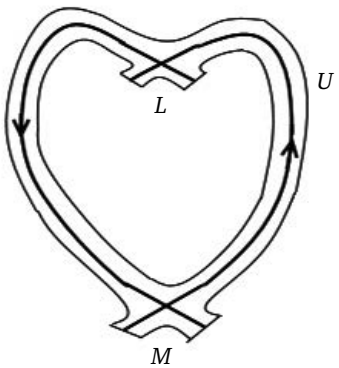


FIGURE 2.2. The neighbourhood $U$.

We assume that the family with parameters $\varepsilon$ and $\delta$ is generic in the sense that

$$\det \begin{pmatrix} \frac{\partial f(0)}{\partial \varepsilon} & \frac{\partial f(0)}{\partial \delta} \\ \frac{\partial g(0)}{\partial \varepsilon} & \frac{\partial f(0)}{\partial \delta} \end{pmatrix} \Bigg|_{\varepsilon=0,\delta=0} \neq 0.$$

This inequation is invariant under changes in the parameters. Once we have shown in Section 3 that $H$ is a Banach manifold, this condition implies that the family intersects $H$ transversally. Then without loss of generality we can assume that the maps $f$ and $g$

are of the form

$$f : \Gamma_1^- \to \Gamma_2^+, \qquad f(x) = \varepsilon - \tilde{f}_{\varepsilon\delta}(x); \tag{5}$$

$$g : \Gamma_2^- \to \Gamma_1^+, \qquad g(x) = \tilde{g}_{\varepsilon\delta}(\delta - x), \tag{6}$$

where $\tilde{f}_{\varepsilon\delta}(0) = \tilde{g}_{\varepsilon\delta}(0) = 0$. Thus, the parameters being zero corresponds to the vector field with locked separatrix connections (see Figure 2.1). Since $f$ and $g$ are diffeomorphisms with respect to $x$ and depend smoothly on $\varepsilon$ and $\delta$, there exist positive smooth functions $a(\varepsilon, \delta)$ and $b(\varepsilon, \delta)$ such that

$$\begin{aligned} \tilde{f}_{\varepsilon\delta}(x) &= a(\varepsilon, \delta)x(1 + o(1)), \\ \tilde{g}_{\varepsilon\delta}(x) &= b(\varepsilon, \delta)x(1 + o(1)) \end{aligned} \tag{7}$$

as $x \to 0$. Moreover, their derivatives satisfy the following relations:

$$\tilde{f}'_{\varepsilon\delta}(x) = a + o(1); \quad \tilde{g}'_{\varepsilon\delta}(x) = b + o(1)\ ; \tag{8}$$

$$\frac{\partial \tilde{f}_{\varepsilon\delta}}{\partial \varepsilon}(x) = \frac{\partial a}{\partial \varepsilon}x(1 + o(1)); \quad \frac{\partial \tilde{g}_{\varepsilon\delta}}{\partial \varepsilon}(x) = \frac{\partial b}{\partial \varepsilon}x(1 + o(1)); \tag{9}$$

$$\frac{\partial \tilde{f}_{\varepsilon\delta}}{\partial \delta}(x) = \frac{\partial a}{\partial \delta}x(1 + o(1)); \quad \frac{\partial \tilde{g}_{\varepsilon\delta}}{\partial \delta}(x) = \frac{\partial b}{\partial \delta}x(1 + o(1)); \tag{10}$$

as $x, \varepsilon, \delta \to 0$. Here, $a, b, \frac{\partial a}{\partial \varepsilon}, \frac{\partial b}{\partial \varepsilon}, \frac{\partial a}{\partial \delta}, \frac{\partial b}{\partial \delta}$ denote the values at $\varepsilon = \delta = 0$ of the functions $a(\varepsilon, \delta)$ and $b(\varepsilon, \delta)$ and of their respective partial derivatives.

Moreover, as the maps $f$ and $g$ depend smoothly on the parameters, the following relations are true:

$$\begin{aligned} a(\varepsilon, \delta) &= a + O(\varepsilon) + O(\delta); \\ b(\varepsilon, \delta) &= b + O(\varepsilon) + O(\delta); \\ \lambda(\varepsilon, \delta) &= \lambda + O(\varepsilon) + O(\delta); \\ \mu(\varepsilon, \delta) &= \mu + O(\varepsilon) + O(\delta). \end{aligned} \tag{11}$$

We recall that a saddle is called *dissipative (non-dissipative)* if its characteristic exponent is strictly greater (less) than 1. Depending on the values of the characteristic exponents of the saddles, six cases are possible:

(1) $\mu > 1, \quad \lambda < 1, \quad \lambda\mu < 1$
(2) $\mu > 1, \quad \lambda < 1, \quad \lambda\mu > 1$
(3) $\mu < 1, \quad \lambda > 1, \quad \lambda\mu > 1$
(4) $\mu < 1, \quad \lambda > 1, \quad \lambda\mu < 1$
(5) $\mu > 1, \quad \lambda > 1$
(6) $\mu < 1, \quad \lambda < 1$

To help the reader appreciate the differences between these 6 cases, we make the following observations. 1) The dissipativity of a saddle determines the behaviour of trajectories passing close to that saddle; in particular, it affects the appearance of limit cycles when the separatrix loops break. 2) The sign of the product $\lambda\mu$ determines the behaviour of the trajectories near both saddles; in particular, it affects the order of the appearance of loops of the separatrices of the saddles.

In what follows we will consider only case (1) (the case of a dissipative and non-dissipative saddle) and case (6) (the case of two non-dissipative saddles), since the remaining cases can be reduced to these two. Indeed, if time is reversed, then case 1 goes to case 3, and case 6 to case 5. Cases 1 and 4 are obtained from each other by renaming $\lambda$ to $\mu$ and vice versa. Cases 2 and 3 are obtained from each other in a similar way. Case 1 corresponds to the bifurcation diagram in Figure 1.2a and case 6 to Figure 1.2b.

We now give the definitions that are necessary to understand Theorems 1 and 2, which we stated in the first section.

**Definition 1.** Two vector fields are called *orbitally topologically equivalent* if there exists a homeomorphism of phase spaces preserving the orientation that takes the trajectories of one vector field to the trajectories of the other.

**Definition 2.** A vector field is called *structurally stable* if there exists a neighbourhood of it in the space of smooth vector fields in which any vector field is orbitally topologically equivalent to the given vector field.

**Definition 3.** The *bifurcation diagram* of a family is the set of all points in the spaces of parameters corresponding to structurally unstable vector fields.

## 3. Vector fields with a 'heart' polycycle as a Banach manifold

Consider a $C^r$-smooth vector field $v \in \mathrm{Vect}^r(\mathbb{S}^2)$ which contains a separatrix connection $\gamma$ of two saddles. Let $SC \subset \mathrm{Vect}^r(\mathbb{S}^2)$ denote the set of $C^r$-vector fields with a separatrix connection and $SC_\gamma$ denote the set of vector fields $w \in SC$ for which the separatrix $\gamma_w$ is close to $\gamma$.

**Theorem 3** (Sotomayor[3])**.** *The set $SC_\gamma$ is a Banach manifold of codimension 1 in the space $\mathrm{Vect}^r(\mathbb{S}^2)$, that is, for any point $w \in SC_\gamma$ there exist a neighbourhood $W \subset \mathrm{Vect}^r(\mathbb{S}^2)$ and a $C^{r-1}$-smooth function $F : W \to \mathbb{R}$ such that*

- *$F^{-1}(0) = SC_\gamma \cap W$,*
- *$DF(p)$ is a surjection for any point $w \in SC_\gamma$.*

The 'heart' polycycle appears as a result of the formation of two separatrix connections. We let $\tilde{H}$ denote the intersection of two surfaces $SC_{\gamma_1}$ and $SC_{\gamma_2}$ corresponding to vector fields with one of these separatrix connections (see Figure 3.1).

**Proposition 1.** *$\tilde{H}$ is a Banach manifold of smoothness class $C^{r-1}$ and codimension 2.*

*Proof.* According to Sotomayor's Theorem, for any vector field $w \in \tilde{H}$ there exist a neighbourhood $W$ and $C^{r-1}$ functions $F_1$, $F_2 : W \to \mathbb{R}$ such that $F_1^{-1}(0) = SC_{\gamma_1} \cap W$ and $F_2^{-1}(0) = SC_{\gamma_2} \cap W$. We have $\tilde{H} \cap W = SC_{\gamma_1} \cap SC_{\gamma_2} \cap W = F_1^{-1}(0) \cap F_2^{-1}(0)$. Therefore $\tilde{H}$ is the zero set of the function $F = (F_1, F_2) : W \to \mathbb{R}^2$. In the proof of his theorem, Sotomayor chose as $F_1$ and $F_2$ functions which put into correspondence with each vector field the unlocking threshold of the separatrix connections on a certain transversal. For the family $V$ with the 'heart' polycycle which is described in later sections, a suitable choice of $F_1$ and $F_2$ is to take the functions $f$ and $g$.

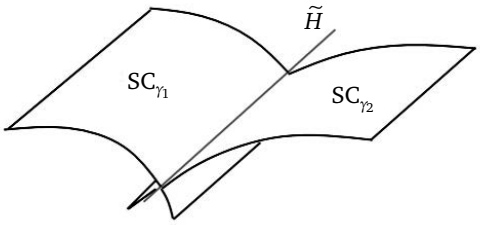


Figure 3.1. The set of vector fields with the 'heart' polycycle is the intersection of two Banach submanifolds.

We will prove that $dF$ is surjective. To do this it is sufficient to find two vectors $h_1, h_2 \in T_w\mathrm{Vect}^r(\mathbb{S}^2)$ such that $dF(h_1)$ and $dF(h_2)$ are linearly independent.

First, we will construct $h_1$. We choose a point $x_0 \in \mathbb{S}$ on the separatrix of the vector field $w$ which defines the surface $SC_{\gamma_1}$. We straighten the vector field in some neighbourhood $Ox_0$ of this point. We take an infinitely smooth vector field $h_1 = (0, \rho(x, y))$,


FIGURE 3.2. a) The offset vector field $h$; b) The resulting vector field $w + \varepsilon h$.

where $\rho(x, y) \geq 0$, which vanishes identically on the whole sphere apart from on $Ox_0$. In this neighbourhood the vector fields $h$ and $w$ are orthogonal. We consider a 1-parameter family of vector fields $w + \xi h$, where $\xi \in (\mathbb{R}, 0)$ (see Figure 3.2). In the straightening chart this family is given by

$$\begin{cases} \dot{x} = 1, \\ \dot{y} = \xi\rho(x, y). \end{cases} \tag{12}$$

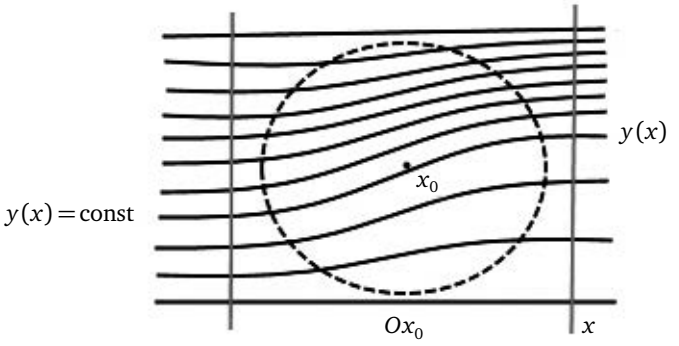


FIGURE 3.3. The vector field $w+\xi h_1$ defined by (12) in the straightening chart for $\xi \neq 0$.

The phase curves $y_\xi(x)$ of this system depend on the parameter $\xi$ (see Figure 3.3). When $\xi = 0$, all phase curves of the system (12) are given by equation $y_0(x) = \text{const}$. Therefore,

$$F_1(w + \xi h) = y_\xi(x) - y_0(x) = \xi \int_{-\infty}^{x} \rho(x, y_\xi)dx - y_0(x). \tag{13}$$

Thus,

$$\frac{\partial}{d\xi} F_1(w + \xi h) = \int_{-\infty}^{x} \rho(x, y_\xi)dx + \xi \int_{-\infty}^{x} \frac{\partial}{\partial\xi}\rho(x, y_\xi)dx.$$

By the theorem which states that the solution depends continuously on the parameter, the second term after the equals sign tends to zero as $\xi \to 0$. Since $\rho$ is nonnegative and is not identically zero on $Ox_0$, hence $\frac{\partial}{d\xi} F_1(w + \xi h) \neq 0$. This inequation is preserved on passing to the original (not straightened) chart. Moreover, $\frac{\partial}{d\xi} F_2(w + \xi h_1) = 0$, because, by construction, the second separatrix does not unlock.

In a similar fashion, we choose a point on the other separatrix and construct the vector field $h_2$. This satisfies $\frac{\partial}{d\xi}F_2(w+\xi h_2) \neq 0$ and $\frac{\partial}{d\xi}F_1(w+\xi h_2) = 0$. Therefore, the image of the differential $F = (F_1, F_2)$ contains two independent vectors $(\frac{\partial}{d\xi}F_1(w+\xi h_1), 0)$ and $(0, \frac{\partial}{d\xi}F_2(w+\xi h_2))$, as required. □

## 4. Passage to the first quadrant

A neighbourhood of any saddle is divided into four hyperbolic sectors. When the parameters are both zero, one of the sectors for both the saddle $M$ and $L$ lies in the connected component of the complement of the polycycle which is distinct from the component containing the other three. We call this sector the *main* sector and the two adjoining it *adjacent* sectors (see Figure 4.1). Notice, that if for small enough values of the parameters, some separatrix enters an adjacent sector of one of the saddles, then it leaves the neighbourhood $U$ of the polycycle. This follows from the construction of the neighbourhood.

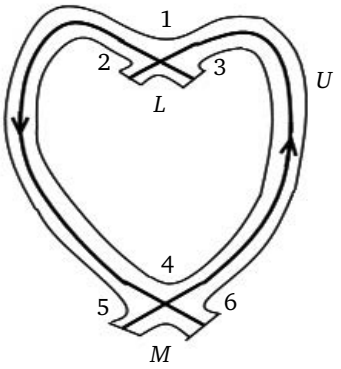


Figure 4.1. For the saddle $L$, the main sector is 1, and the adjacent sectors are 2 and 3. For the saddle $M$, the main sector is 4, and the adjacent sectors are 5 and 6.

**Proposition 2.** *If both the parameters $\varepsilon$ and $\delta$ are non-zero and at least one of them is negative, then the break-up of the 'heart' polycycle does not lead to the appearance of separatrix connections.*

*Proof.* 1) Let $\varepsilon < 0,\ \delta < 0$. The separatrix leaving the saddle $M$ reaches the neighbourhood $U_L$ of the saddle $L$, enters an adjacent sector and therefore leaves the neighbourhood $U$ of the polycycle (see Figure 4.2). Reversing time, the incoming separatrix of the saddle $L$ reaches the neighbourhood $U_M$ of the saddle $M$ and arguing analoguously it also leaves the neighbourhood of the polycycle. The reasoning for the separatrix coming in to $M$ and the separatrix leaving $L$ is exactly the same reversing the time. Therefore, all separatrices leave the neighbourhood $U$.

2) Let $\varepsilon < 0,\ \delta > 0$. As above, if $\varepsilon < 0$ then the separatrix leaving $M$ and the separatrix entering $L$ both leave $U$. The separatrix leaving $L$ reaches the neighbourhood $U_M$ of the saddle $M$, comes into an adjacent sector of it and leaves the neigbourhood of the polycycle. Reversing time, the separatrix entering the saddle $M$ meets $U_L$ and 'moves' along the incoming separatrix of the saddle $L$ until it reaches $U_M$ and leaves the neighbourhood $U$ of the polycycle.

3) Let $\varepsilon > 0,\ \delta < 0$. The proof follows the same lines as in paragraph 2). Thus, we conclude that outside the first quadrant the bifurcation diagram contains only the coordinate axes. □

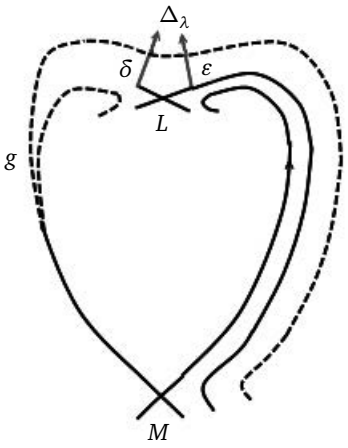


FIGURE 4.2. The vector field in the case when one of parameters is negative.

**Corollary 1.** *If at least one of the parameters is negative, then there are no limit cycles for the corresponding vector field.*

*Proof.* Assume that the vector field contains a limit cycle. Both saddle points cannot be on the same side of the cycle, because each saddle has only one sector such that the trajectories passing through it do not leave the neighbourhood $U$. Moreover, these sectors are located in the polycycle so that the limit cycle passing through them leaves the saddles in different connected components. Therefore, the saddles are separated by the limit cycle and no separatrix of one saddle can reach an adjacent sector of the other saddle, as described in the proof of Proposition 2. Thus, if a limit cycle exists, then both parameters are positive. □

Next we will study the part of the bifurcation diagram inside the first quadrant.

## 5. Separatrix loops

In this section we will describe all the separatrix loops that arise, that is, the homoclinic orbits to the saddles.

**Proposition 3.** *Curves on the bifurcation diagram corresponding to separatrix loops divide the germ of the first quadrant at the origin into three connected components.*

We let $SL_M$ denote the curve in the space of parameters corresponding to vector fields with a separatrix loop of the saddle $M$ and $SL_L$ the one corresponding to the separatrix loop of the saddle $L$. Henceforth we will call the sector between the ordinate axis and the curve $SL_M$ the upper sector, the sector between the axis of abscissas and $SL_L$ the lower sector, and the remaining sector the middle sector.

*Proof.* The following relation is necessary for the birth of a loop near the saddle $M$ (see Figure 5.1b):

$$g \circ \Delta_\lambda \circ f(0) = 0. \tag{14}$$

Denote the expression on the left hand side of (14) by $\Phi(\varepsilon, \delta)$. Note that $\Phi(0, \delta) = g(0) = \tilde{g}_{0\delta}(\delta) > 0$ for all $\delta > 0$, while $\Phi(\varepsilon, 0) = \tilde{g}_{\varepsilon 0}(\Delta_\lambda(\varepsilon)) < 0$ for all $\varepsilon > 0$. Therefore, by continuity, the inequality $\Phi(\varepsilon, \delta) < 0$ holds on the line joining the points $(\varepsilon, 0)$ and $(\varepsilon, \delta)$ for some small $\delta > 0$. Consider an arbitrarily small rectangle $R$ with vertices $(0, 0)$,

$(\varepsilon_0, 0)$, $(\varepsilon_0, \delta_0)$ and $(0, \delta_0)$. For any fixed $\delta$, the function $\Phi(\varepsilon, \delta)$ takes values of opposite signs at the ends of the section $\delta = \text{const}$ of the rectangle $R$. By continuity, any such section contains a point $(\delta, \varepsilon)$ such that $\Phi(\varepsilon, \delta) = 0$. The vector field corresponding to this point contains a separatrix loop of the saddle $M$. Now we prove that on each section this point is unique if $\delta > 0$ is sufficiently small. To do this, it suffices to verify that the rectangle $R$ can be chosen small enough, so that inside it the function $\Phi(\varepsilon, \delta)$ is strictly decreasing with respect to $\varepsilon$, that is $\frac{\partial \Phi}{\partial \varepsilon}(\varepsilon, \delta) < 0$. We will make use of the following lemma.

**Lemma 1.** *Let $h_1(x, \tau_1, \tau_2), h_2(x, \tau_1, \tau_2) : (\mathbb{R}^3, 0) \to (\mathbb{R}^3, 0)$ be $C^1$-smooth functions and let $\Delta_\nu(x, \tau_1, \tau_2) = x^{\nu(\tau_1, \tau_2)}$, where $\nu(\tau_1, \tau_2) \in C^1(\mathbb{R}^2, 0), 0 < \nu(0, 0) < 1$. Suppose that for $x, \tau_1, \tau_2 \to 0$:*

$$\begin{gathered} \frac{\partial h_i}{\partial \tau_j}(x, \tau_1, \tau_2) \to c_{ij}, \text{ where } c_{ij} \neq 0 \Leftrightarrow i = j; \\ \frac{\partial h_i}{\partial x}(x, \tau_1, \tau_2) \to a_i < 0; \\ h_i(x, \tau_1, \tau_2) \to 0. \end{gathered} \tag{15}$$

*Then*

$$\frac{\partial}{\partial \tau_1} h_2 \circ \Delta_\nu \circ h_1(x, \tau_1, \tau_2) \to -\infty$$

*for $x, \tau_1, \tau_2 \to 0$, where composition is with respect to the variable $x$.*

*Proof.* We have:

$$\frac{\partial}{\partial \tau_1} h_2 \circ \Delta_\nu \circ h_1 = \frac{\partial h_2}{\partial \tau_1} + \frac{\partial h_2}{\partial x} \left( \frac{\partial \Delta_\nu}{\partial \tau_1} + \frac{\partial \Delta_\nu}{\partial x} \frac{\partial h_1}{\partial \tau_1} \right). \tag{16}$$

By condition, $\frac{\partial h_1}{\partial \tau_1}(x) \to c_{11} \neq 0$ and $h_1(x) \to 0$; hence the expression in parentheses in (16) is

$$\frac{\partial \Delta_\nu}{\partial \tau_1}(h_1(x)) + \frac{\partial \Delta_\nu}{\partial x}(h_1(x)) \frac{\partial h_1}{\partial \tau_1}(x) = \frac{\partial \nu}{\partial \tau_1} h_1(x)^\nu \ln h_1(x) + \nu h_1(x)^{\nu - 1} \frac{\partial h_1}{\partial \tau_1}(x) \to +\infty$$

for $x, \tau_1, \tau_2 \to 0$. Therefore, according to (15), expression (16) tends to $-\infty$ as $x, \tau_1, \tau_2 \to 0$. □

Now we return to the proof of Proposition 3. From now on we divide it into the following two stages: proving the existence of a curve in the space of parameters which corresponds to the vector fields a) with the loop of the saddle $M$, and b) with the loop of the saddle $L$. The latter stage subdivides further into two: b1) saddles with different dissipativity, which was denoted in Section 2 by case 1; b2) saddles with the same dissipativity, which was denoted by case 6.

a) Set $h_1 = f$, $h_2 = g$, $\Delta_\nu = \Delta_\lambda$, $\tau_1 = \varepsilon$ and $\tau_2 = \delta$; according to (8)–(10), for $\lambda < 1$ the relation (14) is valid both in case 1 (dissipative and non-dissipative saddles) and in case 6 (two dissipative saddles) and the function $\Phi$ from this equation satisfies the conditions of the lemma. Therefore, $\frac{\partial \Phi}{\partial \varepsilon} \to -\infty \neq 0$ as $\varepsilon, \delta \to 0$. Thus, for any section $\delta = \text{const}$ of $R$ there exists a unique point $(\varepsilon(\delta), \delta)$ such that $\Phi(\varepsilon(\delta), \delta) = 0$. Moreover, applying the implicit function theorem to the equation $\Phi(\varepsilon, \delta) = 0$ at the point $(\varepsilon(\delta), \delta)$, for small $\delta > 0$ the function $\varepsilon(\delta)$ is seen to be smooth. Since $R$ can be chosen arbitrarily small, $\varepsilon(\delta) \to 0$ as $\delta \to 0$. Therefore, according to (11), equation (14) can be written as

$$\begin{gathered} \varepsilon(\delta) = \Delta_\lambda^{-1}(\delta) = \delta^{\frac{1}{\lambda(\varepsilon(\delta), \delta)}} = \delta^{\frac{1}{\lambda + o(1)}} \text{ as } \delta \to 0, \\ \ln \varepsilon(\delta) = \tfrac{1}{\lambda}(1 + o(1)) \ln \delta \text{ as } \delta \to 0. \end{gathered} \tag{17}$$

b) Similarly, for the other saddle (see Figure 5.1d):

$$f \circ \Delta_\mu \circ g(0) = 0. \tag{18}$$

Denote the expression on the left-hand side of (18) by $\Psi(\varepsilon, \delta)$. We note that $\Psi(0, \delta) = -\tilde{f}_{0\delta} \circ \Delta_\mu \circ \tilde{g}_{0\delta}(\delta) < 0$ for $\delta > 0$ and $\Psi(\varepsilon, 0) = \varepsilon > 0$. There exists a small rectangle $R$, such that the function $\Psi(\varepsilon, \delta)$ has opposite signs at the endpoints of the section $\varepsilon = \text{const}$. Therefore, by the continuity of $\Psi(\varepsilon, \delta)$, there exists a point on any such section such that the corresponding vector field contains a separatrix loop of the saddle $L$.

b1) Set $h_1 = g$, $h_2 = f$, $\Delta_\nu = \Delta_\mu$, $\tau_1 = \delta$ and $\tau_2 = \varepsilon$; then, according to (8)–(10), for $\mu < 1$ (which is true only in case 6, of two dissipative saddles) the function $\Psi$ from equation (18) satisfies the conditions of the lemma. Therefore, $\frac{\partial \Psi}{\partial \delta} \to -\infty \neq 0$ as $\varepsilon, \delta \to 0$. Thus, by the implicit function theorem applied to the equation $\Psi(\varepsilon, \delta) = 0$ at any point where the solution exists, for small values of the parameters the curve on the bifurcation diagram corresponding to vector fields with the separatrix loop of the saddle $L$ is the graph of a function $\delta(\varepsilon)$ which is smooth for $\varepsilon > 0$. Since the rectangle $R$ is arbitrarily small, then $\delta(\varepsilon) \to 0$ as $\varepsilon \to 0$. Therefore, using (11) we can write equation (18) in the form:

$$\begin{aligned} \delta(\varepsilon) = \tilde{g}_{\varepsilon\delta}^{-1} \circ \Delta_\mu^{-1} \circ \tilde{f}_{\varepsilon\delta}^{-1}(\varepsilon) &= \tfrac{1}{b} \left(\tfrac{\varepsilon}{a}\right)^{\frac{1}{\mu(\varepsilon, \delta(\varepsilon))}} (1 + o(1)), \\ \ln \delta(\varepsilon) = \tfrac{1}{\mu}(\ln \varepsilon - \ln a)(1 + o(1)) &- \ln b + o(1) \end{aligned} \tag{19}$$

as $\varepsilon \to 0$.

b2) Set $h_1 = f^{-1}$, $h_2 = g^{-1}$, $\Delta_\nu = \Delta_\mu^{-1}$, $\tau_1 = \varepsilon$ and $\tau_2 = \delta$; then, according to (8)–(10) from the equation $\Psi^{-1}(0) = 0$, obtained from (18) for $\mu > 1$ (which is only true in case 1 for dissipative and non-dissipative saddles), $\Psi^{-1}$ function satisfies the hypotheses of the lemma. By similar reasoning we conclude that there is a smooth curve in the diagram corresponding to vector fields with separatrix loops of the saddle $L$. We can verify immediately that the asymptotics in this case coincide exactly with (19).

Thus, the bifurcation diagram contains two curves which divide the first quadrant into three sectors. Since $\frac{1}{\mu} > \lambda$, comparing relations (17) and (19), we can conclude that the curve $SL_M$ lies above $SL_L$ on the bifurcation diagram. Proposition 3 is proved. □

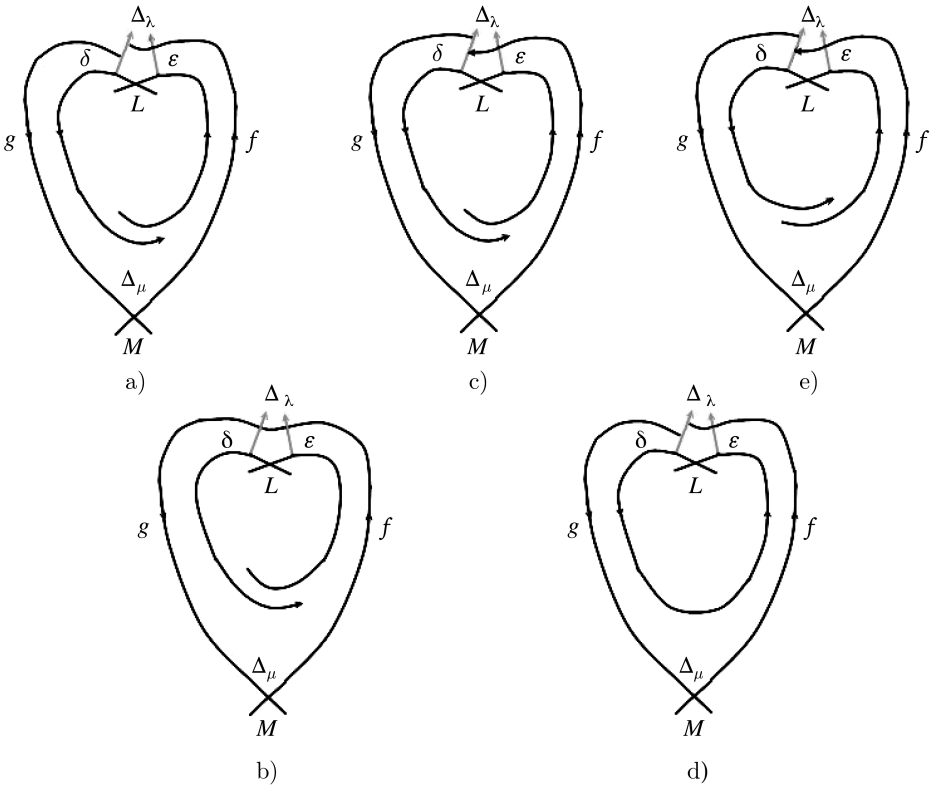


FIGURE 5.1. The phase portrait of the vector field in the a) upper; c) middle; e) lower sectors, as well as at the moment of the birth of the separatrix loops. It shows the processes of birth and death for the separatrix loops as we go from the upper to the lower sector in the order a-b-c-d-e.

## 6. Dissipative and non-dissipative saddles. The bifurcation diagram

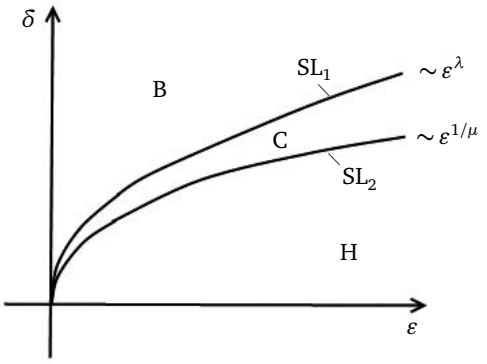


FIGURE 6.1. Curves of the bifurcation diagram which correspond to the separatrix loops. Here B, C and H denote the upper, middle and lower sectors, respectively.

In this section we will look closely at case 1, for which the characteristic exponents of the saddles satisfy the inequalities

$$\mu > 1, \ \ \lambda\mu < 1. \tag{20}$$

We will show that the bifurcation diagram of the family is as given in Fig. (1.2a). Henceforth we take the diagram to be just its germ at zero in the base $(\mathbb{R}^2, 0)$.

### 6.1. **Limit cycles.**

**Proposition 4.** *Parameter values in the upper sector of the bifurcation diagram correspond to vector fields which contain zero, one or two limit cycles in the neighbourhood $U$. In the middle sector there is exactly one limit cycle. Vector fields corresponding to parameter values in the lower sector contain no limit cycles.*

*Proof.* We will find fixed points of the Poincaré map for the 'heart' polycycle (these depend on the parameters). These points correspond to the limit cycles which appear when the polycycle is destroyed. We obtain the equation $\Delta(x) = x$ which, due to (4), can be written

$$\Delta_\lambda \circ f(x) = (\Delta_\mu \circ g)^{-1}(x).$$

The maps on both sides of the equality act from the transversal $\Gamma_1^-$ to the transversal $\Gamma_2^-$. Using (2), (3), (5) and (6) we obtain

$$\Delta_\lambda(\varepsilon - \tilde{f}_{\varepsilon\delta}(x)) = \delta - (\Delta_\mu \circ \tilde{g}_{\varepsilon\delta})^{-1}(x). \tag{21}$$

In view of (20) and (8), the $x$-derivative of the left-hand side of (21) is equal to

$$-\frac{\partial}{\partial y}\Delta_\lambda(y)\Big|_{y=\varepsilon-\tilde{f}_{\varepsilon\delta}(x)} \frac{\partial \tilde{f}_{\varepsilon\delta}(x)}{\partial x} = -\Big(\varepsilon - ax(1+o(1))\Big)^{\lambda-1} a(\lambda + o(1)) \tag{22}$$

as $x, \varepsilon, \delta \to 0$. This derivative tends to $-\infty$ as $x$ tends to the zero of the function $\varepsilon - ax(1+o(1))$ from the left. The $x$-derivative of the right-hand side of (21) is equal to

$$-\frac{\partial}{\partial y}\tilde{g}_{\varepsilon\delta}^{-1}(y)\Big|_{y=\Delta_\mu^{-1}(x)} \frac{\partial \Delta_\mu^{-1}(x)}{\partial x} = -\frac{(1+o(1))}{b\mu} x^{\frac{1}{\mu}-1} \tag{23}$$

as $x, \varepsilon, \delta \to 0$. It tends to $-\infty$ as $x$ tends to zero from the right. It follows that on the segment $[0, \varepsilon]$ for $\varepsilon$ sufficently small, the derivative (22) is decreasing and the derivative (23) is increasing. Therefore, on this segment the function on the left-hand side of (21) is convex upward and the function on the right-hand side is convex downwards.

Thus, the graphs of the functions from the left- and right-hand sides of equation (21) can intersect in at most two points (this follows from Rolle's theorem). If the intersection takes place on the axis of abscissas, then both functions map some point on the transversal $\Gamma_1^-$ into zero on the transversal $\Gamma_2^-$ (see Fig. 6.2d). Therefore, there is a separatrix loop of the saddle $L$. If the intersection takes place on the ordinate axis, then we conclude that both functions map a zero on the transversal $\Gamma_1^-$ into one and the same point on the transversal $\Gamma_2^-$ (see Fig. 6.2b). Therefore there is a loop of the saddle $M$. Thus, Fig. 6.2a corresponds to the upper sector, Fig. 6.2c to the middle and Fig. 6.2e to the lower sector. The vector fields corresponding to Figures 6.2 a, b, c, d, e, are shown on the corresponding Figures 5.1 a, b, c, d, e.

We conclude that there are no limit cycles in the lower sector (see Fig. 6.2e), there is exactly one limit cycle in the middle sector (see Fig. 6.2c), and the number of limit cycles in the upper sector can vary between 0 to 2 (see Fig. 6.2a). Indeed, if the function on the right-hand side of equation (21) behaves like curve 1 in Fig. 6.2a, that is, has two intersection points with the graph of the other function, then the vector field has two limit cycles. If it behaves like curve 2, that is, it is tangent to the other graph at a

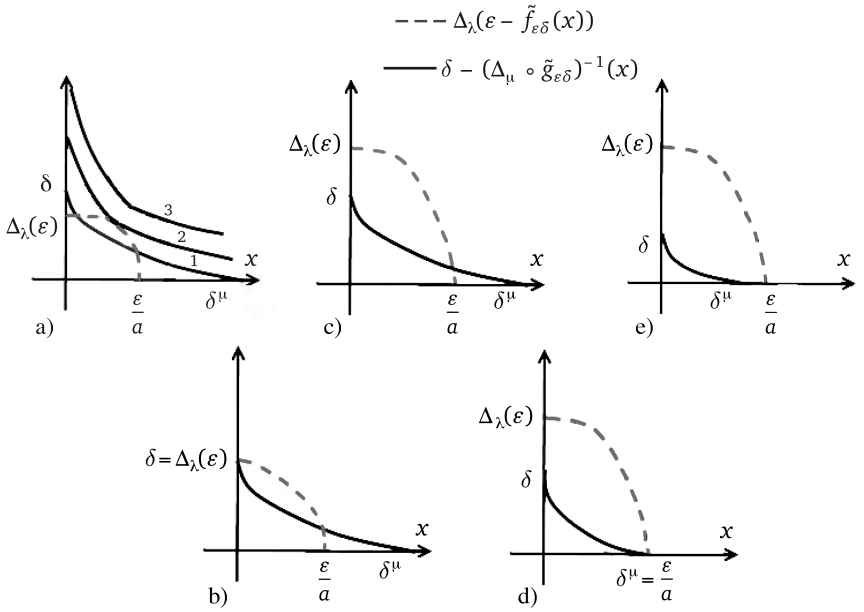


FIGURE 6.2. Plots of two convex functions from the left- and right-hand sides of equation (21) in the sectors: a) lower (no limit cycles); c) middle (one cycle); e) upper (from 0 to 2 cycles). Plots b) and d) correspond to the moment of birth of the separatrix loops of the saddles $M$ and $L$. The values on the axis of abscissas are given up to a factor $(1 + o(1))$ as $\varepsilon, \delta \to 0$. All five pictures demonstrate the appearance of the intersection points of the plots in the process of transition from the upper sector to the lower one in the order a-b-c-d-e.

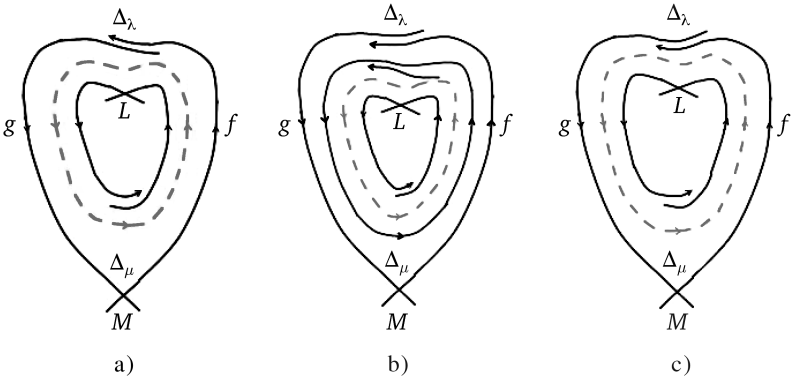


FIGURE 6.3. Limit cycles: a) unstable for a vector field corresponding to parameters from the middle sector; b) stable and unstable for parameters from the upper sector; c) semistable for a vector field corresponding to parameters from the upper sector.

point, then there is one limit cycle. Finally, if it behaves like curve 3, that is, it does not intersect the graph of the other function, then there are no limit cycles. □

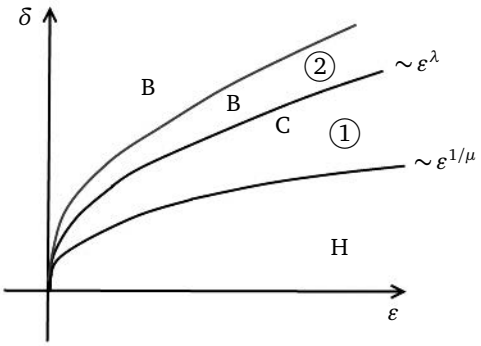


FIGURE 6.4. Upper, middle and lower sectors on the bifurcation diagram and the number of limit cycles of the corresponding vector fields (denoted by Roman numerals).

We conclude that changing the parameter along the vertical line $\varepsilon = \varepsilon_0$ so that $\delta$ increases leads to the following evolution of the phase portrait. In the lower sector there are no cycles, but after the loop of the saddle $L$ breaks down an unstable cycle arises. Then the separatrix loop of the saddle $M$ collapses and a stable limit cycle arises. These cycles approach one another, and eventually merge, momentarily forming a semi-stable limit cycle that disappears as a result of the saddle-node bifurcation.

*Remark.* In section 4.2, when discussing the separatrix loop of the saddle $M$ no mention was made of the fact that the vector field in Figure 5.1b is not shown in its entirety. Enhancing the picture by adding the unstable limit cycle, we obtain the final phase portrait shown in Figure 6.5.

### 6.2. **The emergence of sparkling separatrix connections.**

**Definition 4.** Let $V$ be a local $k$-parameter family of vector fields on the sphere. We consider the separatrix leaving one saddle and the separatrix entering the other saddle and note in the parameter base the set of points at which these separatrices form a separatrix connection. We say that a *series of sparkling separatrix connections* is observed in the family if the germ at the origin of this set is divided into an infinite number of connected components.

In order to describe the sparkling separatrix connections that arise in the family $V$ under study, we prove the following proposition.

**Proposition 5.** *Consider a 1-parameter family $W = \{w_\varepsilon | \varepsilon \in (\mathbb{R}, 0)\}$. Suppose that the vector field $w_0$ has a parabolic limit cycle. Suppose that the Poincaré map $\Delta_\varepsilon$, depending on the parameter $\varepsilon$, defined on a transversal $\Gamma$ to this cycle has no fixed points for $\varepsilon > 0$. Suppose that the vector field $w_0$ has two saddle points, $E$ and $I$, located on different sides of the cycle and that the separatrix leaving the saddle $E$ (separatrix entering the saddle $I$) winds round the cycle in positive (negative) time (see Figure 6.6).*

*Then for small $\varepsilon > 0$ separatrix connections appear in the family $W$: that is, there exists a sequence $\varepsilon_n \to 0$ such that the vector field $w_{\varepsilon_n}$ contains a common separatrix of saddles $E(\varepsilon_n)$ and $I(\varepsilon_n)$ close to $E$ and $I$.*

This result is more general than the Malta–Palis theorem [2] as it does not require that the parabolic cycle be twofold.

*Proof.* Suppose that the transversal $\Gamma$ intersects the cycle at the point 0, intersects the separatrix leaving the saddle $E$ at the point $x_1(\varepsilon)$, and the separatrix of the saddle $I$

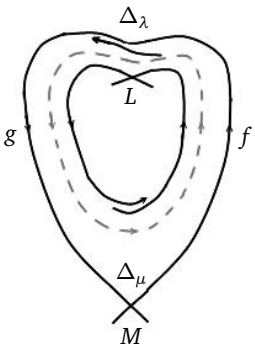


FIGURE 6.5. Phase portrait of the vector field in the case of a separatrix loop of the saddle $M$.

at the point $x_2(\varepsilon)$, and assume that $x_1(0) > 0 > x_2(0)$. Let $\varepsilon > 0$ be arbitrarily small. Since there are no fixed points, $\Delta_\varepsilon(x) < x$ for any $x \in [x_2, x_1]$. Therefore, there exists $n$ such that $\Delta_\varepsilon^{\circ n}(x_1(\varepsilon)) < 0$ and $\Delta_\varepsilon^{\circ -n}(x_2(\varepsilon)) > 0$. But if $\varepsilon = 0$, then the inequalities $\Delta_0^{\circ m}(x_1) > 0$ and $\Delta_0^{\circ -m}(x_2) < 0$ hold for any $m$. Therefore, for any $n$ large enough there exists $\varepsilon_n$ such that $\Delta_{\varepsilon_n}^{\circ n}(x_1(\varepsilon_n)) = \Delta_{\varepsilon_n}^{\circ -n}(x_2(\varepsilon_n))$. □

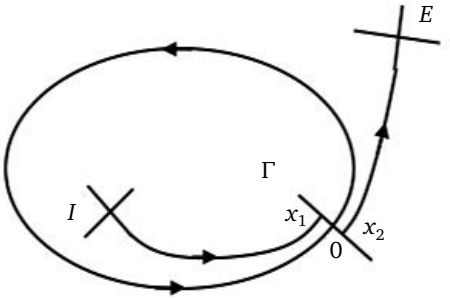


FIGURE 6.6. Semistable limit cycle.

**Proposition 6.** *Consider a 1-parameter family $W = \{w_\varepsilon | \varepsilon \in (\mathbb{R}, 0)\}$. Suppose that the vector field $w_0$ has saddle points $M$ and $I$, with a separatrix loop attached to $M$ and with $I$ inside this loop, and suppose that the separatrix leaving the saddle $I$ winds around the loop from inside in positive time. Suppose that the transversal $\Gamma$ intersects the separatrix leaving the saddle $I$ and the separatrix entering the saddle $M$ at points whose coordinates along the transversal are equal to $x_1(\varepsilon)$ and 0 respectively, and that $x_1(0) > 0$ (see Figure 6.7). Suppose that the parameter-dependent Poincaré map $\Delta_\varepsilon$ on the half-transversal $\Gamma$ to this loop has no fixed points for $\varepsilon > 0$.*

*Then separatrix connections appear in $W$ for small $\varepsilon > 0$. That is, there exists a sequence $\varepsilon_n \to 0$ such that for every $n$ the vector field $w_{\varepsilon_n}$ has saddles $I(\varepsilon_n)$ and $M(\varepsilon_n)$ close to $I$ and $M$, for which $I(\varepsilon_n)$ and $M(\varepsilon_n)$ have a common separatrix.*

*Proof.* Let $\varepsilon > 0$ be arbitrarily small. Since the Poincaré map $\Delta_\varepsilon$ has no fixed points for $\varepsilon > 0$, then $\Delta_\varepsilon(x) < x$ for any $x \in [0, x_1]$. It follows that there exists $n$ for which $\Delta_\varepsilon^{\circ n}(x_1(\varepsilon)) < 0$. But, for $\varepsilon = 0$ the inequality $\Delta_0^{\circ m}(x_1) > 0$ is true for any $m$. Therefore, for any $n$ large enough, $\varepsilon_n$ exists such that $\Delta_{\varepsilon_n}^{\circ n}(x_1(\varepsilon_n)) = 0$. □

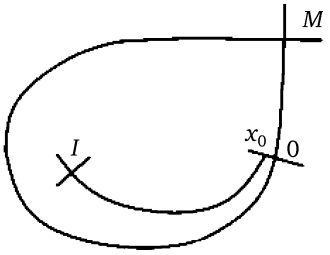


FIGURE 6.7. Separatrix loop.

**Theorem 4.** *For a generic family containing a vector field with the 'heart' polycycle, in case (20) two series of sparkling separatrix connections appear.*

*Proof.* In the middle sector the saddles $M$ and $L$ are separated by a limit cycle, therefore separatrix connections cannot arise. In the upper sector, with the disappearance of the semi-stable limit cycle, there is a Malta–Palis bifurcation [2]. In the lower sector sparkling separatrix connections appear when the separatrix loop of the saddle $L$ breaks up.

In fact, take any curve $\gamma_1$ in the parameter space that intersects the curve corresponding to a semi-stable limit cycle transversally. It determines a 1-parameter family of vector fields. For those values of the parameter for which the curve is above the curve corresponding to the semi-stable limit cycle, there are no limit cycles, and hence this family satisfies the hypotheses of Proposition 5. Thus, when the 'heart' polycycle breaks, the Malta–Palis bifurcation occurs (see Figure 6.8).

Similarly, draw a curve $\gamma_2$ that intersects $SL_L$ transversally. Then it also defines a family satisfying the hypotheses of Proposition 6.

The curves $\gamma_1$ and $\gamma_2$ can come arbitrarily close to the origin, and hence any neighbourhood of the origin contains a value of the parameter corresponding to a vector field having a separatrix connection and making any sufficiently large number of windings. For small parameter values, the separatrix connections do not extend beyond the neighbourhood $U$, and the saddles $M$ and $L$ do not extend outside $U_M$ and $U_L$. Each separatrix connection intersects any transversal several times. We take the segment of the separatrix between the first and last points of its intersection with some transversal and add on the corresponding segment of that transversal. Then we obtain a loop that lies entirely in the neighbourhood $U$. But $U$ is homeomorphic to an annulus and its fundamental group is nontrivial. Consequently, it is impossible to change the winding number of the separatrix connection by a continuous transformation without breaking it. Therefore, by Definition 4, two series of sparkling separatrix connections appear in the family $V$ (see Figure 6.9): in the upper and lower sectors, respectively. □

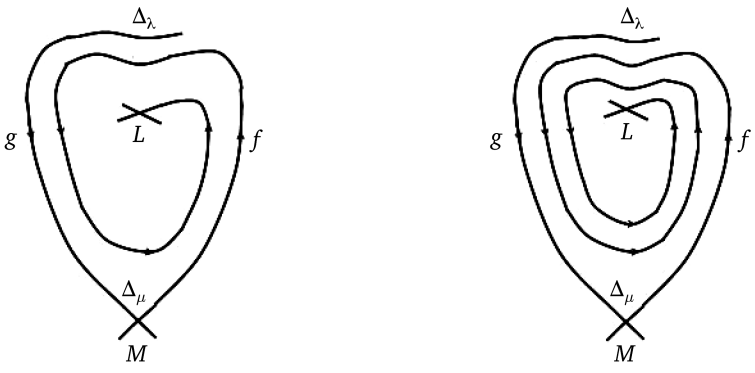


FIGURE 6.8. Sparkling separatrix connections in the upper sector. The separatrix makes a) one b) two windings.

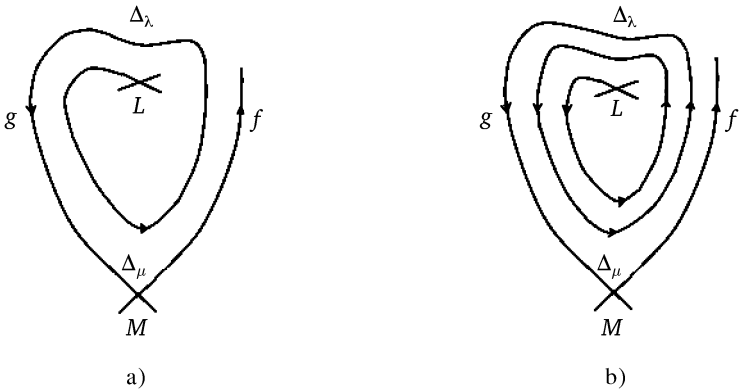


FIGURE 6.9. Sparkling separatrix connections in the lower sector. The separatrix makes a) one b) two windings.

## 7. Two non-dissipative saddles. The bifurcation diagram

Now consider the case when the saddles have the same dissipativity. In Section 2 we showed that we only have to investigate saddles with characteristic exponents satisfying the following inequalities:

$$\mu < 1, \qquad \lambda < 1. \tag{24}$$

### 7.1. **Limit cycles.**

**Proposition 7.** *Suppose that the inequalities (24) hold. Then vector fields corresponding to parameter values in the upper and lower sectors do not have limit cycles. Vector fields corresponding to parameter values in the middle sector have exactly one limit cycle.*

*Proof.* Equation (21) determines the fixed points of the Poincaré map corresponding to limit cycles. If there were a parabolic limit cycle in the family, then there would exist a point $x_0$ such that the equation obtained from (21) by differentiating with respect to $x$ and then setting $x = x_0$ has a solution. We will prove that this equation has no solutions. Differentiating (21) with respect to $x$ and using the expressions (22) and (23) for the derivatives we obtain

$$a(\lambda + o(1))\Big(\varepsilon - ax(1 + o(1))\Big)^{\lambda-1} = \frac{x^{\frac{1}{\mu}-1}}{b\mu}(1 + o(1)) \text{ as } x, \varepsilon, \delta \to 0.$$

Hence

$$\varepsilon = ax(1 + o(1)) + \frac{1}{(ab\lambda\mu)^{\frac{1}{\lambda-1}}} x^{\frac{1-\mu}{\mu(\lambda-1)}}(1 + o(1)) \text{ as } x, \varepsilon, \delta \to 0. \tag{25}$$

Notice that $\frac{1-\mu}{\mu(\lambda-1)} < 0$ by (24). The left-hand side of equation (25) tends to zero as $\varepsilon \to 0$. The right-hand side is the sum of two positive functions and if $x \to 0$, then the second term tends to infinity. Therefore, equation (25) does not have a solution for small $x$, $\varepsilon$ and $\delta$.

If $x$, $\varepsilon$ and $\delta$ are small then the functions on the left- and right-hand sides of (21) are convex upward (see Figure 7.1a). Notice that equation (21) cannot have two solutions (Fig. 7.1b) because, by Rolle's Theorem applied to the difference of these functions, there would exist a point where the values of their derivatives coincide. But this is not possible, because equation (25) for the derivatives has no solution.

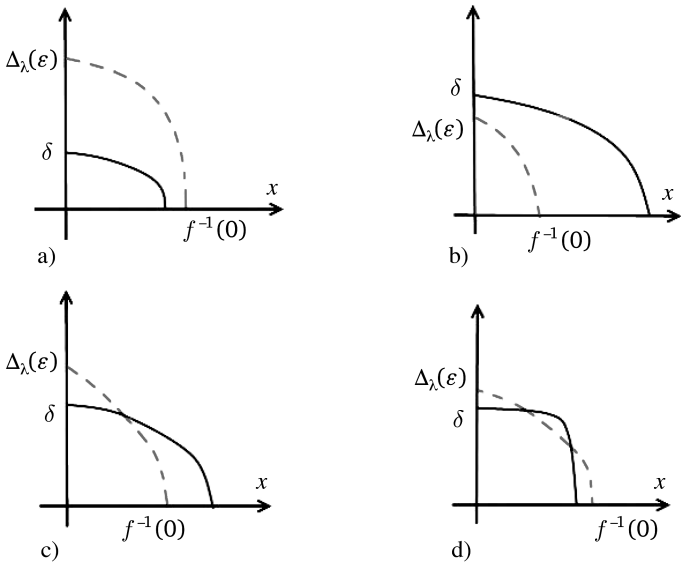


FIGURE 7.1. Graphs of the functions from equation (21): a) in the upper sector; b) in the lower sector; c) possible case in the middle sector; d) impossible case in the middle sector.

Thus, vector fields corresponding to parameter values in the upper and lower sectors do not have limit cycles. For parameters in the middle sector, when one of the separatrix loops breaks up, an unstable limit cycle is born according to (24) and it disappears to form a separatrix loop of the other saddle. □

7.2. **The emergence of sparkling separatrix connections.** Sparkling separatrix connections appear in the upper and lower sectors (see Figures 6.8 and 6.9). In both cases, the connections appear because of the breakup of the separatrix loop. Their appearance is justified by Theorem 4 and similar arguments in the previous section.

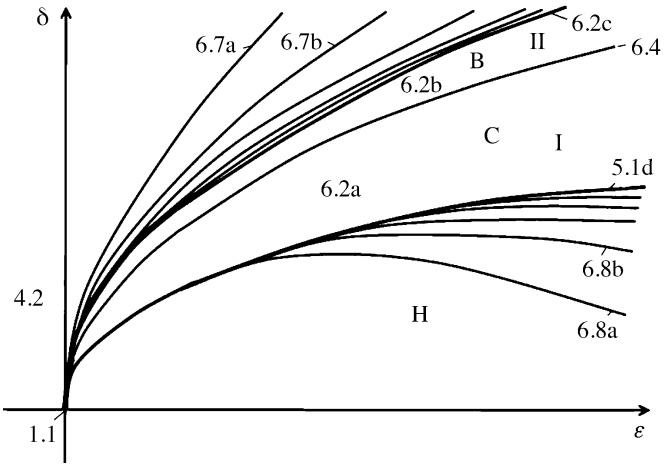


FIGURE 8.1. Bifurcation diagram in case (20). Roman numerals denote the number of limit cycles, Arabic numerals refer to the figure where the corresponding vector field is represented.

## 8. The bifurcation diagram

We will prove Theorems 1 and 2.

*Proof.* According to Proposition 2 and Corollary 1 there are no points, apart from the coordinate axes, outside the first quadrant of the bifurcation diagram which correspond to vector fields with separatrix connections or parabolic limit cycles.

According to Proposition 3, the first quadrant is divided into three sectors by two curves which correspond to vector fields with separatrix loops. According to Proposition 4, in the case of a dissipative or non-dissipative saddle (case 1), in the upper sector there is a curve going out from zero that corresponds to vector fields having a parabolic limit cycle. In the case of two non-dissipative saddles (case 6), there are no parabolic limit cycles. By Theorem 4 and Propositions 5 and 6, there are two series of an infinite number of curves going out from the origin, which correspond to two series of sparkling separatrix connections. Curves of the series in the upper sector accumulate to a curve corresponding to vector fields with a parabolic cycle (case 1) or a separatrix loop of the saddle $M$ (case 6). The curves of the series in the lower sector accumulate to a curve corresponding to vector fields with a separatrix loop of the saddle $L$ (in both cases).

It only remains to show that at all other points in the parameter space the vector fields are structurally stable. Indeed, by the Andronov–Pontryagin Theorem [6], a vector field on a two-dimensional sphere is structurally unstable if and only if there is either a separatrix connection, or a parabolic limit cycle, or a singular point that has an eigenvalue whose real part vanishes. Separatrix connections and limit cycles were considered above. In the neighbourhood $U$, there are no nondegenerate singular points apart from $M$ and $L$. Thus, Theorems 1 and 2 are proved. □

The bifurcation diagram is illustrated in case 1 by Fig. 8.1 and in case 6 by Fig. 8.2.

*Remark* 1. In this paper, the question of the smoothness of curves on the bifurcation diagram corresponding to fields with sparkling separatrix connections has not been touched on. This question, posed in a more general case for arbitrary polycycles, may become the subject of a future paper.

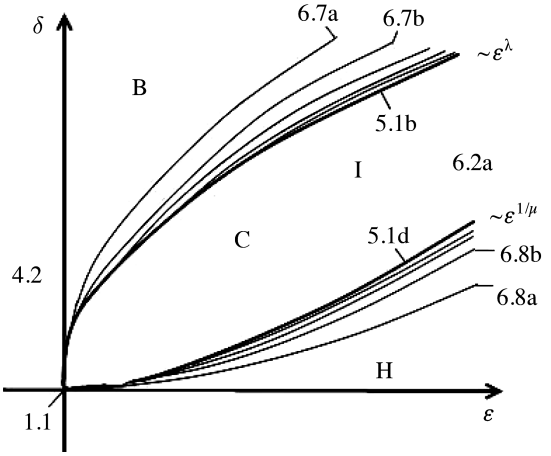


FIGURE 8.2. Bifurcation diagram for case (24).

## REFERENCES

[1] Yu. S. and Weigu Li, *Nonlocal bifurcations*, Moscow, MCCME, 2016. Electronic edition. ISBN 978-5-4439-2322-2, 327–335. [In Russian]

[2] I. P. Malta.and J. Palis, *Families of vector fields with finite modulus of stability*, Lecture Notes in Math., Vol. 898, Springer Verlag, Berlin–New York, 1981. 212–229. MR654891

[3] J Sotomayor,*Generic one-parameter families of vector fields on two-dimensional manifolds*, Inst. Hautes Études Sci. Publ. Math.,**43:43**(1974), 5–46. MR0339279

[4] Yu. Il'yashenko, Yu. Kudryashov and I. Schurov, *Global bifurcations in the two-sphere: a new perspective*, Invent. Math. **213:2**(2018), 461–506. DOI: 10.1007/s00222-018-0793-1. MR3827206

[5] A. Kotova and V. Stanzo, *On few-parameter generic families of vector fields on the two-dimensional sphere. Concerning the Hilbert 16th problem.* AMS Transl. Ser. 2, vol. 165; Adv. Math. Sci., vol. 23, 55–201. Providence, RI: AMS, 1995. MR1334343

[6] A. A. Andronov and L. S. Pontryagin, *Structurally stable systems*, Doklady Akad Nauk, **14:5**(1937),247–250.

DEPARTMENT OF MECHANICS AND MATHEMATICS, MOSCOW STATE UNIVERSITY
*Email address*: sunts_andrew@mail.ru

Translated by IAN MARSHALL
Originally published in Russian